

MIT Open Access Articles

Validation of Computational Fluid-Structure Interaction Analysis Methods to Determine Hydrodynamic Coefficients of a BOP Stack

The MIT Faculty has made this article openly available. **Please share** how this access benefits you. Your story matters.

Citation: Venuturumilli, Raj et al. "Validation of Computational Fluid-Structure Interaction Analysis Methods to Determine Hydrodynamic Coefficients of a BOP Stack." ASME 2015 34th International Conference on Ocean, Offshore and Arctic Engineering, May 31–June 5, 2015, St. John's, Newfoundland, Canada, ASME, 2015. © 2015 by ASME

As Published: <http://dx.doi.org/10.1115/OMAE2015-41198>

Publisher: American Society of Mechanical Engineers (ASME)

Persistent URL: <http://hdl.handle.net/1721.1/108384>

Version: Final published version: final published article, as it appeared in a journal, conference proceedings, or other formally published context

Terms of Use: Article is made available in accordance with the publisher's policy and may be subject to US copyright law. Please refer to the publisher's site for terms of use.



**VALIDATION OF COMPUTATIONAL FLUID-STRUCTURE INTERACTION ANALYSIS
METHODS TO DETERMINE HYDRODYNAMIC COEFFICIENTS OF A BOP STACK**

Raj Venuturumilli
BP America
Naperville, IL, USA

Michael Tognarelli
BP America
Houston, TX, USA

Samir Khanna
BP America
Naperville, IL, USA

Michael Triantafyllou
MIT
Cambridge, MA, USA

ABSTRACT

Drilling riser systems are subjected to hydrodynamic loads from vessel motions, waves, steady currents and vortex-induced motions. This necessitates a proper structural analysis during the design phase using techniques such as finite element analysis (FEA). Common approaches within the FEA packages approximate the individual components including BOP/LMRP (Blow-Out Preventer/Lower Marine Riser Package), subsea tree and wellhead using 2D or 3D beam/pipe elements with approximated effective mass and damping coefficients. Predicted system response can be very sensitive to the mass, hydrodynamic added mass and drag of the large LMRP/BOP/Tree components above the wellhead. In the past, gross conservative estimates on the hydrodynamic coefficients were made and despite this, design criteria were generally met. With the advent of large sixth-generation BOP stacks with the possibility of additional capping stacks, such approximations are no longer acceptable. Therefore, the possibility of relying on the more detailed capability of computational fluid-structure interaction (FSI) analysis for a better calculation of these coefficients is investigated. In this paper, we describe a detailed model developed for a 38:1 scaled down BOP and discuss the subsequent predictions of the hydrodynamic coefficients. The model output is compared against the data from the concurrent tests conducted in an experimental tow tank. The comparison demonstrates that computational FSI can be an effective and accurate tool for calculating the hydrodynamic coefficients of complex structures like BOPs.

INTRODUCTION

Global drilling riser / wellhead / conductor systems are subject to hydrodynamic loads from vessel motions, waves, steady currents and vortex-induced vibration. Design analyses of these are normally performed using finite element analysis (FEA) packages. Within these packages the drilling riser systems are modelled using 2D or 3D beam/pipe finite elements. Geometrically complex looking components such as

BOP/LMRP (Blow-Out Preventer/Lower Marine Riser Package), subsea tree and wellhead are also modelled as beams with a pipe cross-section. In order to accurately predict the response of the system, the physical, structural and hydrodynamic aspects of each component within the system need to be correctly represented in the numerical model.

System resonance can be very sensitive to the mass, hydrodynamic added mass and drag of the large LMRP/BOP/Tree components above the wellhead. In the past, gross conservative estimates on the hydrodynamic coefficients were made and despite this, design criteria were generally met. With the advent of large sixth-generation BOP stacks with the possibility of additional capping stacks, such approximations are no longer acceptable. Therefore, detailed and state-of-the-art computational fluid dynamics based analytical approaches are gaining a foothold in determining these coefficients [1, 2]. Concurrent model tests can be used in blind comparisons to benchmark the calculations.

In the present work, a 38:1 scaled down model of a BOP is chosen to study both computationally and experimentally. Experiments were conducted in a tow-tank at Massachusetts Institute of Technology (MIT). A high fidelity computational model was built using the commercial computational fluid dynamics software. The next few sections describe the FSI model layout, the modelled scenarios and discuss the obtained results while comparing and contrasting against the measured data.

NOMENCLATURE

- L Height of the BOP
- D Diameter of a cylinder with height L and volume equal to that of the BOP
- A Amplitude of the BOP motion
- C_D Drag coefficient
- C_L Lift coefficient
- C_{LV} Coefficient of lift in phase with velocity

- U Free stream speed
- F_x Net force in the stream wise direction
- F_y Net force in the cross-stream direction
- t time elapsed
- k Turbulent kinetic energy

- ρ Water density
- θ Free stream flow angle w.r.t. the BOP
- ω Angular frequency of motion or specific dissipation rate

COMPUTATIONAL MODEL

In keeping with the experimental setup, a model was developed to reproduce the MIT towing tank conditions. The water filled portion of the tank has the following dimensions, 8' x 3' x 2.5' (Figure 1). The model BOP is situated vertically 13.5 cm above the floor of the numerical tow tank. Along its length, the end closer to BOP is treated as a velocity inlet while the other end is treated as a pressure outlet. All other sides except the top surface are treated as walls with no-slip boundary conditions imposed. The top surface, which represents the free surface, is treated as a shear-free wall. Hence, it is assumed, for the sake of keeping the model complexity manageable, that any free surface undulations in the experiments are ignored in the model. This is not an unreasonable assumption given that the clearance above the BOP top to free surface is over 16 cm.

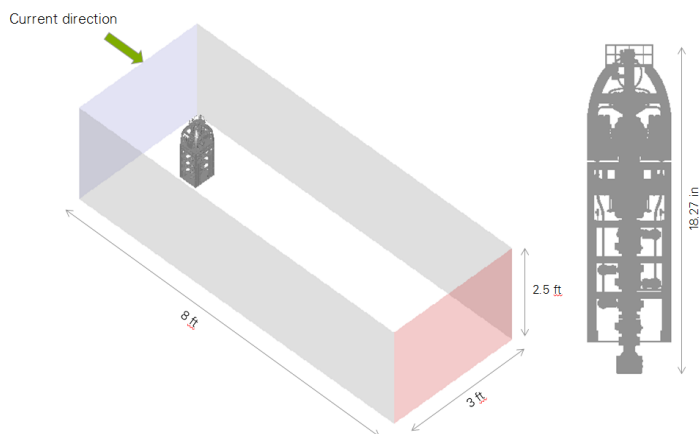


Figure 1. Layout of the computational domain with dimensions shown.

Hydrodynamic properties of a structure are largely governed by the skin friction, surface pressure distribution and vortex shedding aspects of the flow. Hence, it is of paramount importance to take sufficient care to enable the model to capture these effects. This, in turn, means that a sufficient mesh resolution must be maintained in the key areas as well as use appropriate turbulence models that can capture the transient vortex shedding.

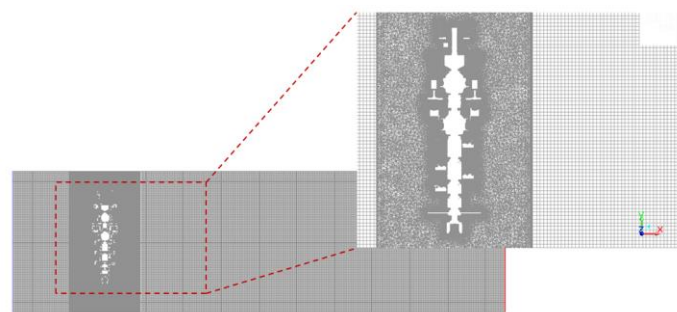


Figure 2. Hybrid (tetrahedral-hexahedral) mesh used for the BOP FSI model.

Commercial Computational Flow Dynamics (CFD) software, ANSYS FLUENT 15.0, was used to develop the transient BOP models. A hybrid mesh consisting of unstructured tetrahedral cells in a cylindrical region surrounding the BOP and structured hexahedral in the region outside (Figure 2) was generated. 6-8 prism boundary layers are used on all BOP surfaces in order to maintain a good mesh resolution as required by the turbulence models. Due to the geometric complexities involved with the model the overall mesh size is quite large at about 64 million control volumes.

Second order accurate numerical schemes are used for both spatial and temporal discretization. Details of the typical numerical methods used for solving the Navier-Stokes equations can be found in [3, 4]. Maximum time step size of 5 ms is used for all the calculations. Various turbulence models were tested on a simplified flow past a cylinder of same volume and height as that of the BOP. Tested turbulence models include $k-\epsilon$, $k-\omega$, Reynolds stress model (RSM), scale adaptive simulation (SAS), detached eddy simulation (DES) [5]. It was found that the predicted drag coefficient is closer to the reported experimental value with the RSM, SAS, DES models while it is under predicted with other models. However, the wake structure looked most realistic, comprising of the spanwise instabilities and a detailed spectrum of vortical structures, with the DES approach. Hence, DES approach is chosen for the BOP model simulations. $k-\omega$ SST model is used as the Reynolds Averaged Navier Stokes (RANS) near wall

blending model with the DES approach. In all the simulated cases, wall y^+ values are maintained at < 5 .

In the cases with BOP oscillation, a moving deforming mesh (MDM) model was used to impose the prescribed rigid body motion to the BOP and to dynamically adjust the mesh as the shape of the computational domain changes.

STEADY TOWING CASES

A set of steady current cases at different inlet flow angles, θ (0° , 22.5° , 45° , 67.5° , 90°) are run. Figure 3 shows the flow angle nomenclature, i.e. BOP orientation relative to the free stream current. It can be seen that the porosity of the BOP structure and the overall width of obstruction to the flow change considerably with the orientation. A steady current of 0.2 m/s is imposed through the inlet. Calculated drag coefficient at different θ captured the measured trend quite well while the actual values are under predicted by $< 20\%$ as shown in Figure 4. Some amount of under prediction of drag coefficient compared to MIT data is anticipated because of the additional structural components present in the tow-tank to hold the BOP in place.

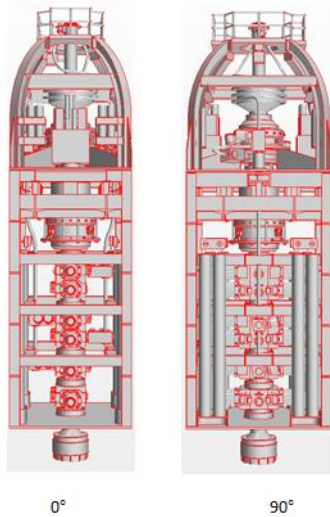


Figure 3. BOP orientation nomenclature with respect to the inflow current (current direction is out of the screen/paper).

Computational FSI models not only calculate the bulk quantities such as drag and added mass but also resolve the entire flow structure around the BOP. This helps to understand such aspects as the wake structure, modes of vortex shedding, flow acceleration effects etc. For example, Figure 5 shows the instantaneous wake of the considered BOP in a steady current of 0.2 m/s at three different inflow angles. It is evident that the wake is highly unsteady with a complex pattern of vortices that get transported downstream. This, in turn, leads to a highly non-uniform velocity distribution in the wake region. At $\theta = 0^\circ$ the wake is narrower because of the reduced obstruction area encountered by the oncoming flow.

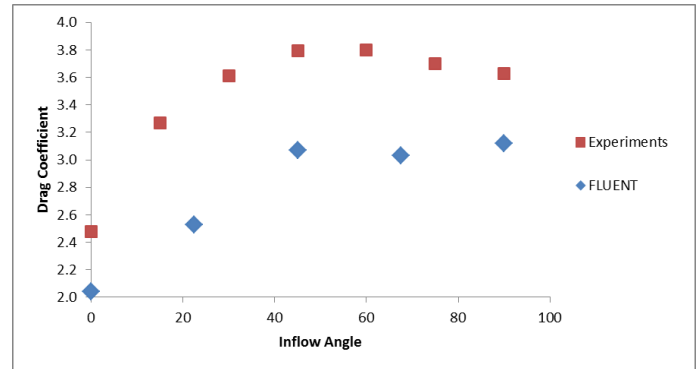


Figure 4. Predicted and measured drag coefficient as a function of the inflow angle.

FORCED OSCILLATION WITH CURRENT

In the next phase, the BOP was given a sinusoidal motion transverse to a steady current of 0.2 m/s and the hydrodynamic coefficients are calculated. Two different amplitudes, $A/D = 0.05, 0.1$, are tested at three different $\theta = 0^\circ, 45^\circ, 90^\circ$. The two amplitudes chosen correspond to the smallest and the largest values used by MIT in their physical model testing experiments. In all the cases frequency of oscillation is set to be 0.907 Hz . Instantaneous wake structure at the three angles at $A/D = 0.1$ is shown in Figure 6. As anticipated, the observed instantaneous wake structure exhibited similar structure as in the previous phase of steady current without oscillation. However, the wake now also oscillates in the spanwise direction with certain frequencies as discussed later. The amplitude of oscillation is small enough not to significantly impact the macroscopic wake characteristics. Drag (in-line with the current), lift in phase with velocity (transverse to the current) and added mass coefficients (transverse to the current) are calculated as shown in Annex A (under subheading A1.1).

As seen from Figure 7 and Figure 8, model results compared quite well against experimental data qualitatively and quantitatively drag coefficient is under predicted by about 17% and added mass is over predicted by about 20% or less for the most data points. In addition to the drag and added mass coefficients, the coefficient of lift in phase with velocity is also calculated. For the $38:1$ model scale BOP under the studied conditions C_{LV} values are all found to be negative, indicating that the BOP would not undergo vortex-induced vibrations (VIV).

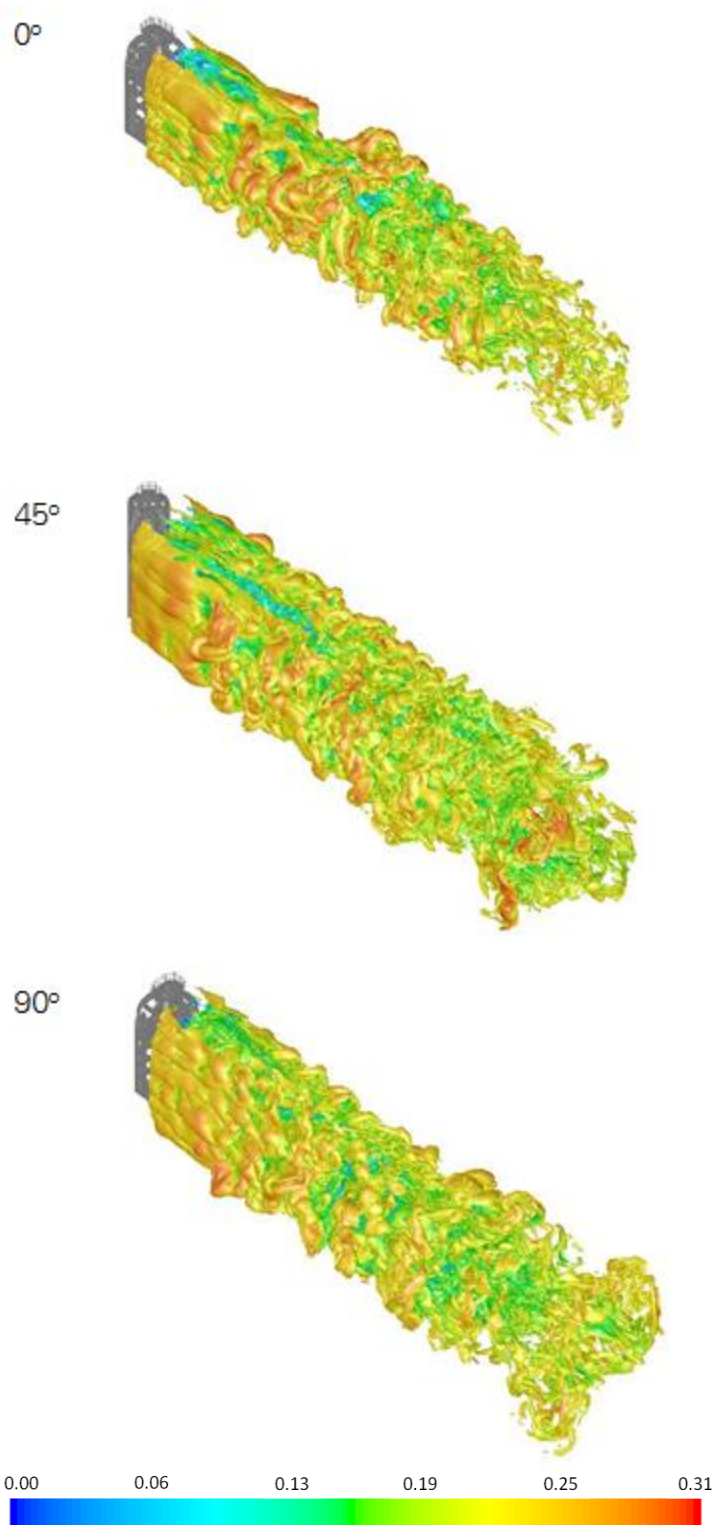


Figure 5. Instantaneous wake structure for steady towing cases at three different inflow angles. Contours represent iso-vorticity surfaces colored by local velocity magnitude (m/s).

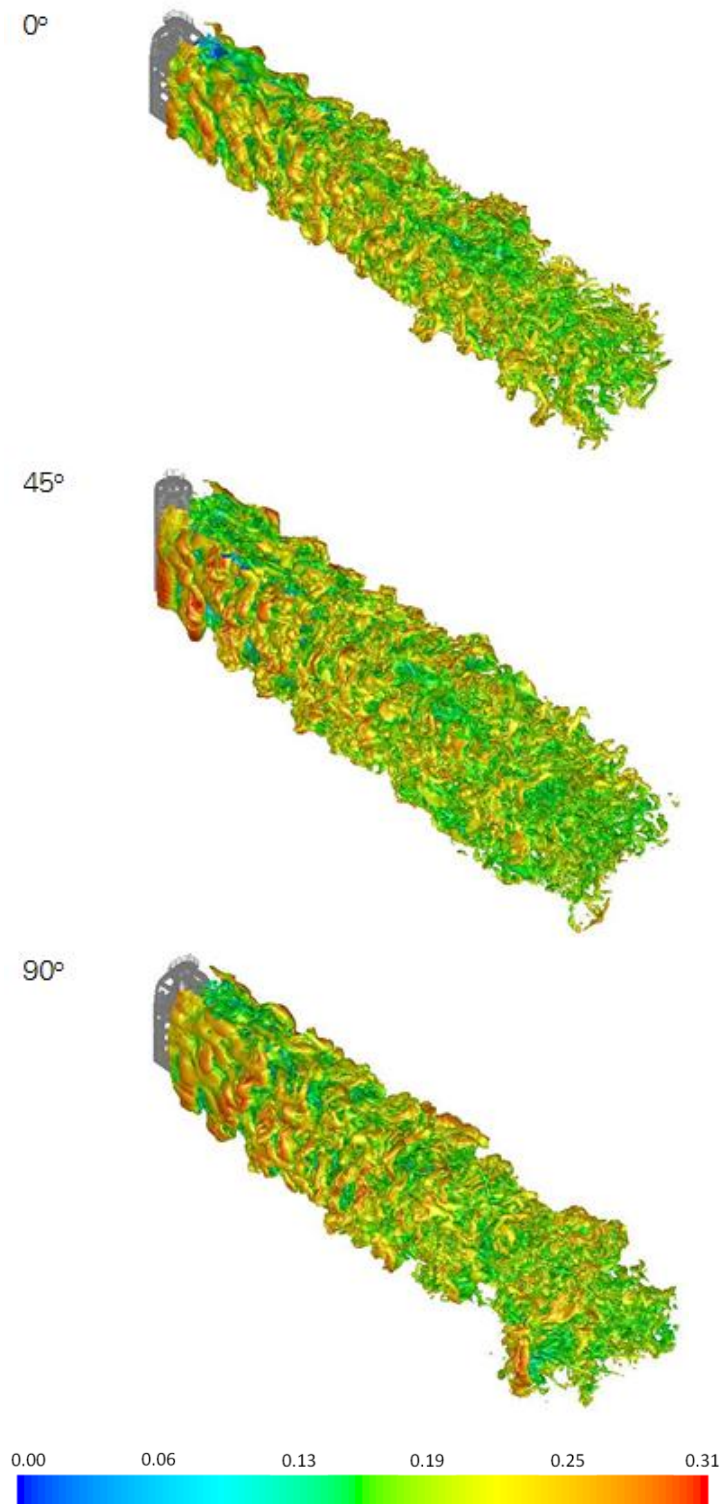


Figure 6. Instantaneous wake structure for forced oscillation cases with steady current of 0.2 m/s at three different angles (m/s).

Drag versus time plots for these cases, as shown in Figure 9, reveal that the drag coefficient oscillates with frequencies other than just the forced oscillating frequency. This is because of the oscillations of the wake due to vortex shedding. Fast Fourier transform of these time series reveal the dominant frequencies as shown in Figure 10. The first two harmonics are close to the forcing frequency and twice the forcing frequency for 0° and 90° . The distinct behavior in the 45° case may be associated with the fact that a relatively sharp corner of the BOP is directed towards the current, rather than a “face” as in the other two cases. This may lead to a distinct oscillatory behavior of the aggregate wake that result in relatively greater dominance of the forcing frequency.

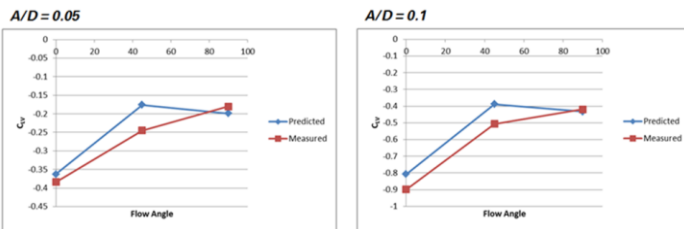


Figure 7. Coefficient of lift in phase with velocity (C_{L_v}) for forced oscillation cases with steady current of 0.2 m/s.

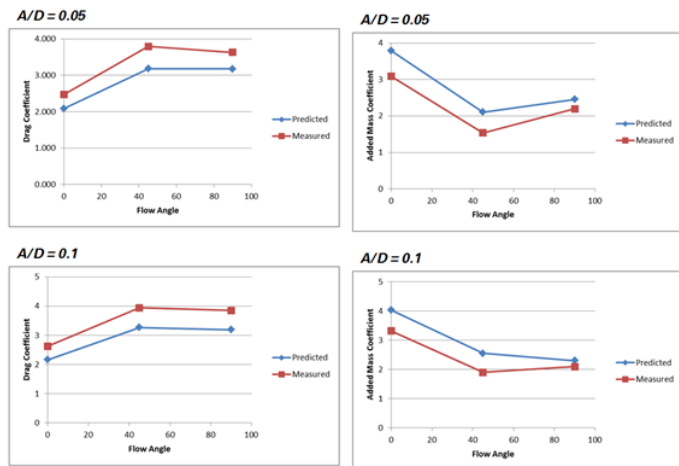


Figure 8. Drag (left) and added mass (right) coefficients for forced oscillation cases with steady current of 0.2 m/s.

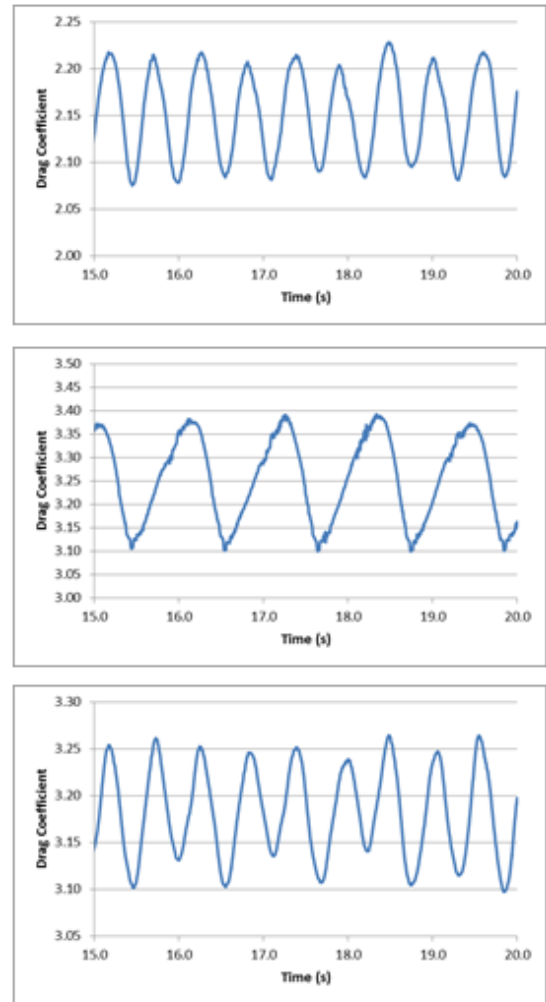


Figure 9. Drag versus time for forced oscillation cases with steady current of 0.2 m/s at three different angles, 0° (top), 45° (middle), 90° (bottom).

FORCED OSCILLATION WITHOUT CURRENT

In the last phase of the study, hydrodynamic effects due to forced oscillation in the absence of a free stream current are investigated. This means the BOP oscillates essentially in its own wake. Again, as before, two amplitudes, $A/D = 0.1$ and $A/D = 0.2$, which correspond to the two ends of the experimental test matrix are chosen. Three different BOP orientations, 0° , 45° , 90° , are considered. In all the cases frequency is again set to be 0.907 Hz. Drag and added mass coefficients aligned with the motion are calculated as shown in Annex A (under subheading A1.2). Once it is ensured that a somewhat periodic pattern in the monitored quantities is obtained, the last 5-10 cycles are analyzed to obtain the hydrodynamic coefficient data.

Figure 11 shows the calculated drag and added mass coefficients and compares them against the MIT measured values. It can be seen that the computational model predictions are again qualitatively in agreement with the experimental data and quantitatively, the disagreement is less than seen in the previous cases (15% or less for the most data points). Figure 12 shows the transverse force experienced by the BOP because of the fluid as a function of time. First, not surprisingly, the frequency of the force variation matched the forcing frequency and secondly, the magnitude of the force doubles as the amplitude is doubled. In the absence of any free stream current, therefore, the linear forces arising from the forced vibrations dominate the hydrodynamics.

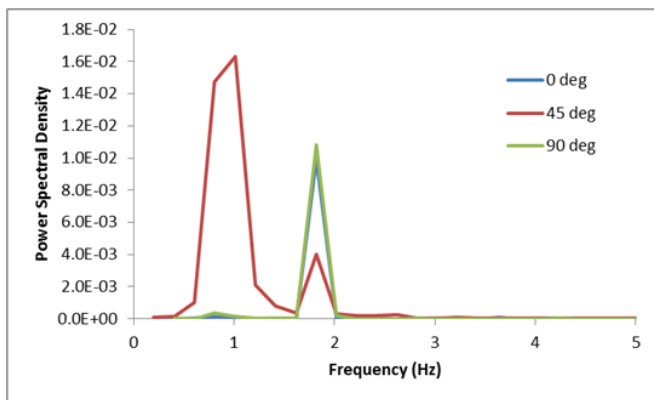


Figure 10. Dominant frequencies in the drag coefficient variation with time for the forced oscillation cases with steady current of 0.2 m/s.

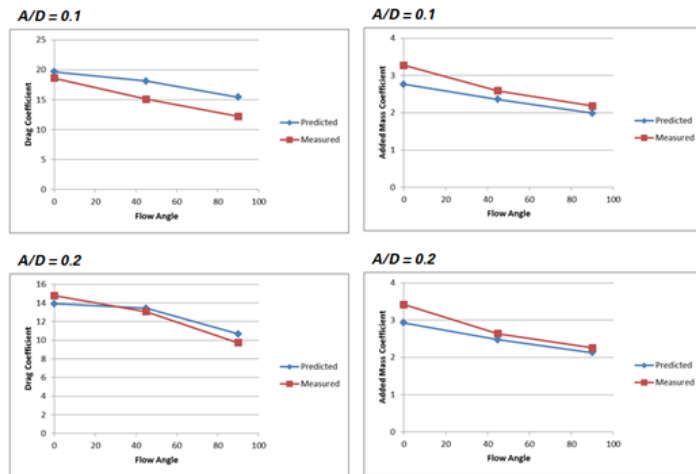


Figure 11. Drag (left) and added mass (right) coefficients for forced oscillation cases without current.

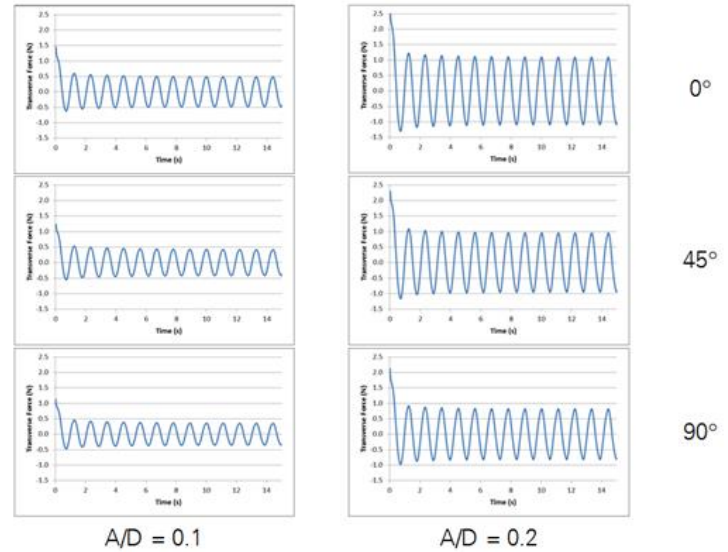


Figure 12. Transverse (sway) force on the BOP as a function of time for forced oscillation cases without current.

CONCLUSIONS

A detailed computational model for the 38:1 model scale BOP is developed and a variety of tow tank conditions are investigated. The developed model closely mimics the MIT tow tank setup. The wake structure is resolved with a good deal of accuracy using detached eddy simulation (DES) turbulence model. Hydrodynamic forces acting on the BOP are predicted and compared with the measured data. Broadly, three sets of cases are simulated as follows: steady tow tank conditions at 0.2 m/s free stream current, transverse BOP oscillation under steady current of 0.2 m/s, transverse BOP oscillation without current. In all these sets different BOP orientations of 0°, 45°, 90° considered. In all the simulated cases good qualitative agreement with the measured data is observed while varying degrees of quantitative disagreement between 2% and 30% is observed. A further analysis into the experimental and numerical uncertainties is necessary to better understand the root cause of these departures. In any case, the study shows that a carefully developed computational FSI model can predict the hydrodynamic forces on complex subsea structures with reasonable fidelity and hence, can be used as a predictive tool.

ACKNOWLEDGMENTS

The authors gratefully acknowledge the BP Global Wells Organization for supporting this work and allowing its publication.

REFERENCES

1. M. J. Stahl, H. S. Pordal, and J. O. Andersen, Computational Fluid Dynamics Analysis as Applied to the

Prediction of Dynamic Hookload Variation in Deepwater Drilling Risers, Proceedings of Offshore Technology Conference, Houston Texas, USA, 2-5 May 2011.

2. W. I. Koolhof, and S. Chai, Numerical Study of the Hydrodynamic Properties of a Mid-Water Arch, Proceedings of the Twenty-second (2012) International Offshore and Polar Engineering Conference, Rhodes, Greece, June 17–22, 2012.
3. S. V. Patankar, Numerical Heat Transfer and Fluid Flow, Hemisphere, 1980.
4. J. H. Ferziger and M. Peric, Computational Methods for Fluid Dynamics, 2nd edition, Springer-Verlag, New York, 1999.
5. ANSYS FLUENT 15.0, Theory Guide, ANSYS Inc., Canonsburg, PA, USA, 2009.

ANNEX A

HYDRODYNAMIC COEFFICIENT DETERMINATION METHOD

For the cases with forced oscillation, a sinusoidal profile for the displacement of the BOP is given as follows,

$$y(t) = \cos(\omega t)$$

During the calculation surge and sway forces on the BOP structure are monitored with time. The drag, lift in phase with velocity and added mass coefficients are calculated using the following approaches.

A1.1 WITH FREE STREAM CURRENT

$$c_D = \frac{F_x}{\frac{1}{2} \rho U^2 dL} \quad c_{lv} = \frac{\frac{2}{T} \int_0^T F_z(t) v(t) dt}{\sqrt{\frac{2}{T} \int_0^T v(t)^2 dt}}$$
$$c_M = \frac{4}{\pi d^2 L \rho} \frac{\int_0^T F_z(t) a(t) dt}{\int_0^T a(t)^2 dt}$$

Where, F_x, F_z are the forces in streamwise & transverse directions

$$a(t) = -A\omega^2 \cos(\omega t), \quad (\text{imposed acceleration})$$

$$v(t) = -A\omega \sin(\omega t), \quad (\text{imposed velocity})$$

ρ, U, D, L are the fluid density, steady current speed, equivalent BOP diameter and BOP height respectively. Integrals are taken over an integer number of oscillation periods.

A1.2 WITHOUT FREE STREAM CURRENT

$$c_D = \frac{\frac{1}{T} \int_0^T F_z(t) v(t) dt}{\frac{2}{3\pi} \rho DL (A\omega)^3}$$
$$c_M = \frac{\frac{1}{T} \int_0^T F_z(t) a(t) dt}{\frac{\pi}{8} \rho D^2 L (A\omega^2)^2}$$

Where, F_z is the force in transverse direction

$$a(t) = -A\omega^2 \cos(\omega t), \quad (\text{imposed acceleration})$$

$$v(t) = -A\omega \sin(\omega t), \quad (\text{imposed velocity})$$

ρ, U, D, L are the fluid density, steady current speed, equivalent BOP diameter and BOP height respectively. Integrals are taken over an integer number of oscillation periods.